Laser Doppler imaging, revisited

Michael Atlan, Michel Gross

HAL Id: hal-00261654
https://hal.science/hal-00261654

Submitted on 14 Mar 2008

Laser Doppler imaging, revisited

M. Atlan, M. Gross

Laboratoire Kastler-Brossel, UMR 8552 (ENS, CNRS, UMPC), Ecole Normale Supérieure, 10 rue Lhomond F-75231 Paris cedex 05

We present a detection scheme designed to perform laser Doppler imaging in a wide-field configu-
ration, aimed at slow flows characterization. The optical field which carries a spectral information
about the local scatterers dynamic state that results from momentum transfer at each scattering
event, is analyzed in the temporal frequencies domain. The setup is based on heterodyne off-axis
digital holography.

The imaging technique presented here is a laser
Doppler scheme in an off-axis holographic configuration.
A heterodyne optical mixing configuration on a CCD
camera is used to select and enhance a tunable frequency
component of the probe light to measure its Doppler
linewidth. Holography is an established scheme in parti-
cle field diagnosis (13) and velocimetry (14; 16). Off-axis
holographic particle velocimetry (HPV) was reported to
be superior to inline HPV in terms of signal-to-noise ra-
tio (SNR) (8) and is the subject of recent developments
(9). We intend to demonstrate that off-axis holography
is also a valuable candidate for laser Doppler linewidth
measurements, which are demanding in terms of SNR. In
conventional laser Doppler velocimetry (LDV), scattered
light coming from a point focused onto a sample is de-
tected by a single detector and analyzed by a spectrum
analyzer. The power spectrum of coherent monochro-
matic light scattered by moving particles is broadened
as a result of momentum transfer. The Doppler shift for
one scattering event is (18) :

$$\omega_D = (\mathbf{k_s} - \mathbf{k_i}) \cdot \mathbf{v} \qquad (1)$$

where $\mathbf{k_i}$ is the incident wave vector, $\mathbf{k_s}$ the scattered
wave vector and $\mathbf{v}$ the scatterer instantaneous velocity.
The resulting broadening of light is linked to the velocity
distribution of scatterers (1; 3). The detection sensitivity
can be improved by homodyne or heterodyne amplifi-
cation which consists in mixing scattered light with a
local oscillator (LO) (4). Doppler maps can be realized
by scanning the focus point on the sample surface,
which constitutes the principle of scanning laser Doppler
Imaging (LDI). The instrument presented here uses an
optical heterodyne mixing scheme on an array detector
to perform quantitative, parallel, wide-field LDI. Con-
trarily to Fourier transform spectroscopy schemes, the
measurement is done directly in the temporal frequency
domain by detuning the LO frequency and measuring
one spectral point at a time.

The experimental setup is based on an optical inter-
ferometer sketched in fig. 1(a). A CW, 80 mW, 780 nm
Sanyo DL-7140-201 diode provides the main laser beam
(field E_L, angular frequency ω_L). A small part of this
beam is split by a prism to form a reference beam (local
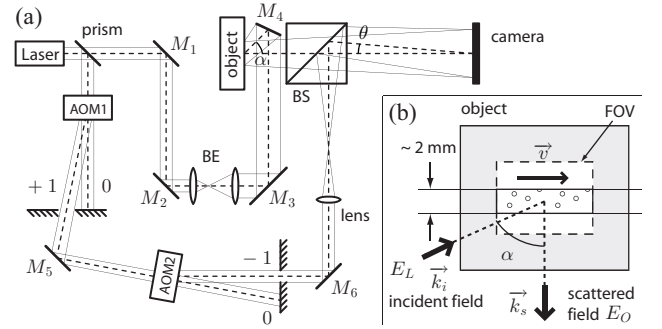oscillator, LO), while the remaining part is expanded

FIG. 1 (a) Setup. M_1 to M_6: mirrors; BS: beam splitter;
BE: beam expander; AOM1 , AOM2: acousto-optic modula-
tors (Bragg cells); -1, 0, +1 : diffraction orders. (b) object
and optical configuration. FOV: field of view. α: scatter-
ing angle. $\mathbf{v}$: flow direction. $\mathbf{k_i}$: incident wave vector. $\mathbf{k_s}$:
scattered wave vector, in the direction of the receiver. E_L:
laser (incident) field. E_O: field scattered by the object. E_{LO}:
reference (local oscillator) field.

and illuminates the object with an average incidence
angle α. The field scattered by the object, E_O, is mixed
with the LO field E_{LO} and detected by a PCO PixelFly
1.3 Megapixel CCD camera (square pixels, pixel size:
6.7 μm, framerate $\omega_S/2\pi = 8$ Hz), set at a distance $d =$
50 cm from the object. Two Bragg cells (acousto-optic
modulators, AOM, Crystal Technology) are used to
shift the LO by a tunable frequency. A 10 mm focal
length lens is placed in the reference arm in order
to create an off-axis ($\theta \approx 1°$ tilt angle) virtual point
source in the object plane (see fig. 1(a)). This configura-
tion constitutes a lensless Fourier holographic setup (12).

To perform an heterodyne detection of the component
of the object field at frequency $\omega = \omega_L + \Delta\omega$, the LO
field E_{LO} is adjusted at frequency $\omega_{LO} = \omega_L + \Delta\omega - \omega_S/n$
with $n > 2$ (typically $n = 4$). The $\Delta\omega$ shift allows the
LO field to match the part of the object field shifted by
$\Delta\omega$ (i.e. their combination produces a static interference
pattern), while the additional shift ω_S/n provokes a
modulation of the interference pattern at ω_S/n, which is
slow enough to be sampled by the CCD camera (the beat
frequency ω_S/n fulfil the sampling theorem condition
$\omega_S/n < \omega_S/2$).

The incident (laser) field is noted:

$$E_{\mathrm{L}}(t) = E_{\mathrm{L}}(\omega_{\mathrm{L}}) \exp(i\omega_{\mathrm{L}}t) \qquad (2)$$

The part of the scattered (object) field shifted at ω (as a consequence of momentum transfer), is:

$$E_{\mathrm{O}}(t) = E_{\mathrm{O}}(\omega_{\mathrm{L}} + \Delta\omega) \exp\left[i(\omega_{\mathrm{L}} + \Delta\omega)t\right] \qquad (3)$$

The LO field is :

$$E_{\mathrm{LO}}(t) = E_{\mathrm{LO}}(\omega_{\mathrm{L}} + \Delta\omega - \frac{\omega_{\mathrm{S}}}{n})$$
$$\times \exp\left[i(\omega_{\mathrm{L}} + \Delta\omega - \frac{\omega_{\mathrm{S}}}{n})t\right] \qquad (4)$$

The intensity I detected by the camera can be expressed as a function of the complex fields (2) :

$$I(t) = |E_{\mathrm{O}}(t) + E_{\mathrm{LO}}(t)|^2 \qquad (5)$$

The part of I modulated at ω_{S}/n (also called heterodyne term) takes the following form:

$$I_{\frac{\omega_{\mathrm{S}}}{n}} = E_{\mathrm{LO}}^*(\omega_{\mathrm{L}} + \Delta\omega - \frac{\omega_{\mathrm{S}}}{n})E_{\mathrm{O}}(\omega_{\mathrm{L}} + \Delta\omega) \exp(i\omega_{\mathrm{S}}t/n) \qquad (6)$$

Note that the LO field amplitude can be considered as constant in the range of frequency shifts of this study ($|\Delta\omega| < 2\,\mathrm{kHz}$). Let's define $A = |E_{\mathrm{LO}}(\omega_L + \Delta\omega - \omega_{\mathrm{S}}/n)|^2$. The complex amplitude of the considered heterodyne term $E_{\mathrm{LO}}^*(\omega_{\mathrm{L}} + \Delta\omega - \omega_{\mathrm{S}}/n)E_{\mathrm{O}}(\omega_{\mathrm{L}} + \Delta\omega)$ constitutes the *heterodyned* object field distribution (OFD). Its power S is:

$$S(\Delta\omega) = A |E_{\mathrm{O}}(\omega_{\mathrm{L}} + \Delta\omega)|^2 \qquad (7)$$

This quantity is read-out from a sequence of n images recorded by the camera. The squared amplitude of the ω_{S}/n frequency component of $I(t)$, calculated by a numerical Fourier transform of the n-image sequence, is proportional to $S(\Delta\omega)$. The modulation/demodulation scheme, described here, is based on the frequency-shifting technique (7). It is the dynamic equivalent of the phase-shifting digital holography technique (10; 17). The lensless Fourier holographic setup (12) is less demanding in numerical calculations than the general Fresnel holography configuration. The numerical reconstruction algorithm of the image is limited to one discrete Fourier transform (11; 15). The artefacts due to the finite size of the sensor and the spatial discrete Fourier transform are narrower than one pixel in the reconstructed image (6), and hence can be neglected.

$S(\Delta\omega)$ is proportional to the spectral power density of the signal field integrated in the frequency window $\Delta\omega \pm \omega_{\mathrm{S}}/2n$. We define the signal S_{dB} represented on spectra profiles and spatial maps as :

$$S_{\mathrm{dB}}(\Delta\omega) = 10 \log_{10}\left[\frac{S(\Delta\omega)}{N(\Delta\omega)}\right] \qquad (8)$$

where $N(\Delta\omega)$ is the quantity $S(\Delta\omega)$ assessed in a region of the reconstructed hologram where the object light contribution is null. It was reported to be close to shot-noise (5).

The sample designed for the experiment consists in a ~ 2 mm-wide canal carved out from a 127 μm parafilm (TM) layer sandwiched between two 1 mm-thick cover-glasses (see fig. 1(b)). This sample was set in front of a white sheet of paper, used to scatter incident light in the direction of the detector. A 1.5% volumic concentration aqueous suspension of latex beads of 1.04 μm of diameter, is perfused in the sample with constant flow thanks to a motorized syringe. A Mie algorithm [1] was used to assess its optical parameters : the scattering coefficient is $\mu_s = 43.6\,\mathrm{mm}^{-1}$, and the anisotropy coefficient is $g = 0.9$. The suspension of latex beads was perfused through the canal of the first sample at several flow rates. The average incidence angle α of the laser beam (see fig. 1(b)) is $\sim 45°$. In this experiment, $S(\Delta\omega)$ maps were realized for $\Delta\omega$ in the [-2.048 kHz, +2.048 kHz] range with $n = 4$ and spacing interval of 8 Hz. $S(\Delta\omega)$ was averaged over m images for each frequency point. One whole spectral cube measurement took ~ 8 minutes and 30 seconds (= 8 images $\times$ 513 frequency shifts $\times$ 1/8 second exposure time), and one spectral point was acquired in 1 second. A steady flow was thus required here for the chosen span and spacing of measured Doppler shifts.

In fig. 2a, the detection is tuned far enough ($\Delta\omega/(2\pi) = -2.048\,\mathrm{kHz}$) where neither statically nor dynamically scattered light should be observed, to measure the noise contribution (< 1 dB). In fig. 2b, the detection is tuned at the maximum of the Doppler shifted and broadened light distribution $\Delta\omega/(2\pi) = -304\,\mathrm{Hz}$ (see fig. 3 c). In fig. 2c, the detection is tuned at a small frequency shift ($\Delta\omega/(2\pi) = -8\,\mathrm{Hz}$) to map very slow velocities. This map reveals an exaltation of small velocities at the border of the canal region, in the absence of any wetting layer. In fig. 2d, the detection is tuned at null frequency shift ($\Delta\omega/(2\pi) = 0\,\mathrm{Hz}$) to measure backscattered light (~ 16 dB) from the static background.

Spectra were calculated in two different regions of the image. The background area and the canal area. The spectrum of light scattered by the background produces the tight peak centered at null frequency shift (fig. 3(a)). It can be interpreted as a measurement of the instrumental linewidth. In the canal area spectra at three flow rates were realized: the first flow rate was null (fig. 3(b)). The observed symmetric spectral broadening is attributed to brownian motion of the latex particles. The second flow rate was $2.2 \times 10^{-4}\,\mathrm{ml.s}^{-1}$, which would correspond to a uniform particle velocity

---

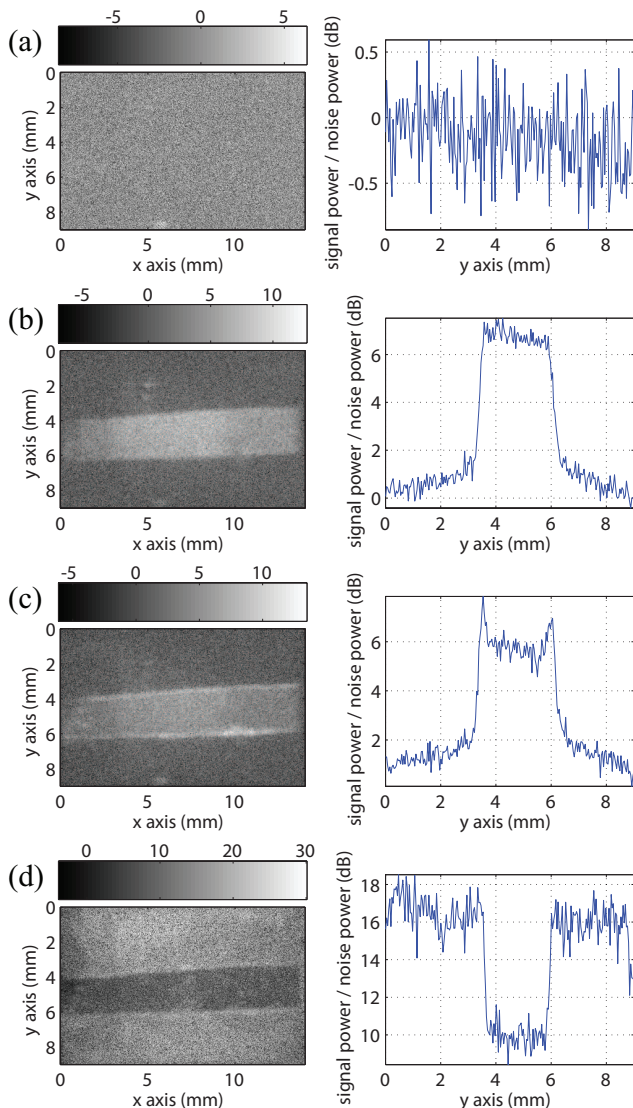[1] http://omlc.ogi.edu/calc/mie_calc.html

FIG. 2 Results obtained with the sample perfused with average velocity v_1. Left: $S_{\mathrm{dB}}(\Delta\omega)$ Right : profiles at $x = 8$ mm. (a) $\Delta\omega/(2\pi) = -2.048\,\mathrm{kHz}$. (b) $\Delta\omega/(2\pi) = -304\,\mathrm{Hz}$. (c) $\Delta\omega/(2\pi) = -8\,\mathrm{Hz}$. (d) $\Delta\omega/(2\pi) = 0\,\mathrm{Hz}$.

$v_1 = 870\,\mu\mathrm{m.s}^{-1}$. The corresponding spectrum is represented on fig. 3(c). The full width at half maximum (-3 dB) of the Doppler peak is ~ 1500 Hz. The third flow rate was $4.4 \times 10^{-4}\,\mathrm{ml.s}^{-1}$, which would correspond to a uniform particle velocity of $v_2 = 1.74\,\mathrm{mm.s}^{-1}$. The corresponding spectrum is represented on fig. 3(d), which shows a broader Doppler peak than in the previous case. Note that we were unable to measure spectral signatures beyond ± 2 kHz. This suggests an intrinsic restriction of the presented instrument to the characterization of small flows.

In conclusion, the presented setup performs a parallel measurement of the power spectrum of scattered monochromatic light. The presented scheme is different from conventional time-domain measurements.
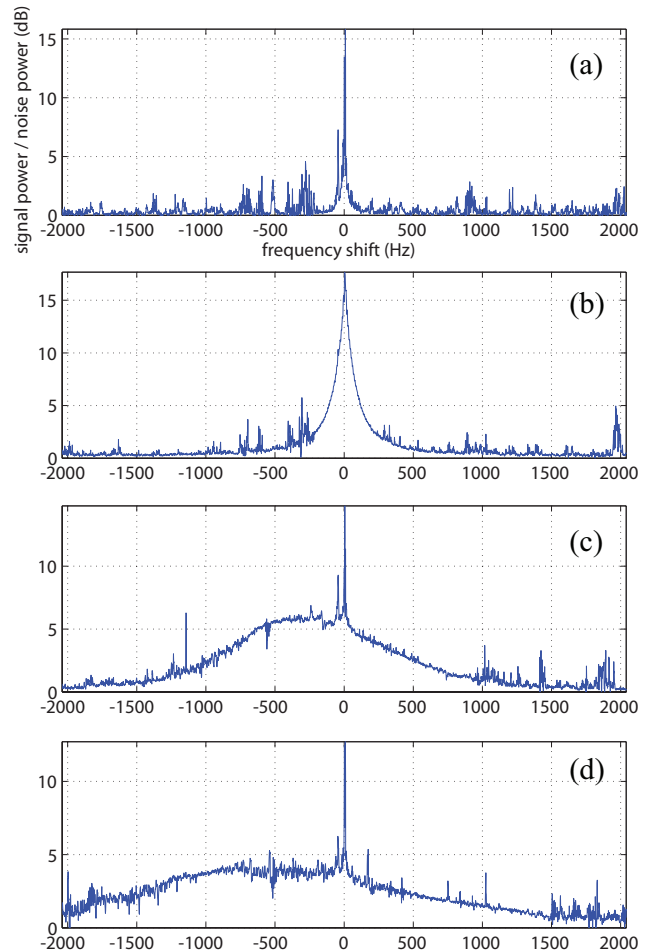

FIG. 3 (a) S_{dB} spectrum of the static background region (frequency-domain instrumental response function). (b, c, d) S_{dB} average spectra in the canal region. (b) Null average velocity. (c) $v = v_1$. (d) $v = v_2 = 2v_1$

Basically, each pixel on a camera acts as an heterodyne photodetector that samples Doppler-shifted light. Each frequency point of the spectrum is acquired at a time, by detuning the LO frequency. The frequency resolution is given by the heterodyne bandwidth of the detection (the inverse of the acquisition time of the n-image sequence), hence the potential suitability for microflow diagnosis (bioflow, microfluidics). Furthermore, the optical configuration allows one to measure algebraic Doppler shifts since we can spatially discriminate the two heterodyne terms in the recorded hologram.

References

[1] R. Bonner and R. Nossal. *Applied Optics*, 20:2097–2107, 1981.

[2] M. Born and E. Wolf. Pergamon Press, 6 edition, 1993.

[3] J. A. Briers. *JOSA A.*, 13:345, 1996.

[4] R. Brown. *Applied Optics*, 40:4004, 2001.

[5] M. Gross, P. Goy, and M. Al-Koussa. *Optics Letters*, 28:2482–2484, 2003.

[6] Thomas M. Kreis. *Optical Engineering*, 41(4):771–778, 2002.

[7] F. LeClerc, L. Collot, and M. Gross. *Optics Letters*, 25(10):716–718, 2000.

[8] H Meng and F Hussain. *Appl. Opt.* , 34:1827–+, April 1995.

[9] Hui Meng, Gang Pan, Ye Pu, and Scott H Woodward. *Measurement Science and Technology*, 15(4):673–685, 2004.

[10] U. Schnars and W. Juptner. *Appl. Opt.*, 33:179–181, 1994.

[11] U. Schnars and W. P. O. Juptner. *Meas. Sci. Technol.*, 13:R85–R101, 2002.

[12] George W. Stroke. *Applied Physics Letters*, 6(10):201–203, 1965.

[13] BJ Thompson, JH Ward, and WR Zinky. *Applied Optics*, 6(3):519, 1967.

[14] JD Trolinger, RA Belz, and WM Farmer. *Appl. Opt.*, 8(5):957, 1969.

[15] Christoph Wagner, Sonke Seebacher, Wolfgang Osten, and Werner Juptner. *Applied Optics*, 38:4812–4820, 1999.

[16] LM Weinstein, GB Beeler, and AM Lindemann. *American Institute of Aeronautics and Astronautics*, AIAA-526, 1985.

[17] I. Yamaguchi and T. Zhang. *Optics Letters*, 18:31, 1997.

[18] Y. Yeh and H. Z. Cummins. *Appl. Phys. Lett.*, 4:176–179, 1964.